

# Chapter 2

## Review of experimental methods

This chapter gives a brief description of the techniques used for the main investigations carried out for the purpose of this thesis. Basic principles and the outlines of the basic functionality of the setups are presented.

### 2.1 Photoluminescence Spectroscopy (PL)

#### 2.1.1 Introduction

Photoluminescence (PL) spectroscopy is a very efficient, contactless, nondestructive, widely used technique for the analysis of the optoelectronic properties of semiconductors, which requires very little sample manipulation. Photoluminescence is defined as the spontaneous emission of light from a material under optical excitation and can be therefore used to provide detailed information on discrete electronic states involving both intrinsic optical processes and about the wide variety of defect which are endemic in practical semiconductor materials and extrinsic optical processes ( internal transitions involving defects and their energy levels) by applying an external light with energy  $h\nu \gtrsim E_G$ , where  $E_G$  denotes the energy band gap, and observing the re-emitted photons [40, 41]. The main uses of photoluminescence are:

- Understanding of recombination mechanisms: Analysis of photoluminescence helps to understand the underlying physics of recombination processes;
- Identification of surface, interface, and impurity levels,
- Band gap determination: Most common radiative transitions in semiconductors occur between states in the conduction and valence bands, with the energy difference known as band gap  $E_G$ ;
- Assessment of the material quality: Material quality can be measured by quantifying the amount radiative recombination, keeping in mind that non-radiative recombination is associated to localized defect levels that are detrimental to material quality and subsequently to device performance
- Detection of defect and impurity levels: Radiative transitions can also involve localized defects and the photoluminescence energy associated to these levels can be used to identify these specific defects.

However photoluminescence has some fundamental drawbacks such as:

- Study of deep states: The inefficiency of studies of recombination mechanisms at very deep centres, where any radiative transitions give very broad spectra due to strong phonon coupling;
- Non- radiative processes: Its reliance only on radiative processes makes materials with weak radiative activities (low quality indirect band gap) very difficult to study.

## 2.1.2 Radiative transitions in semiconductors

### 2.1.2.1 Free excitons (Ex)

A free electron in the conduction band can bind a free hole in the valence band in an hydrogen-like system by its Coulombic field as a pair of opposite charges and form a composite quasi-particle named exciton. In the case that the exciton is not trapped by any defect or impurity, it is called a free exciton. Hence, the new neutral carrier created is a free exciton and when it recombines, the corresponding energy of the photon emitted is given by

$$E_{exc} = E_g - \frac{2\pi^2 m_r^* e^4}{h^2 \epsilon^2} \frac{1}{n^2}$$

where  $E_g$  is the band gap energy,  $h$  Planck's constant,  $\epsilon$  is the dielectric constant,  $m_r^*$  the reduced effective mass of the electron-hole pair,  $n$  is an integer indicating the various allowed states of the free excitons. The second term of the equation is the inner binding energy of the exciton. There are several possible discrete binding energies of excitons. The ground state corresponds to  $n = 1$ , and excited states correspond to  $n = 2, 3, \dots$ . In turn the reduced mass is given by

$$\frac{1}{m_r^*} = \frac{1}{m_e^*} + \frac{1}{m_h^*}$$

where  $m_e^*$  and  $m_h^*$  are the effective masses of electrons and holes, respectively.

### 2.1.2.2 Bound excitons (Bx)

Bound excitons involve the recombination process of electron transitions from the conduction band to neutral acceptor levels ( $e, A^\circ$ ) and electron transitions from neutral donor levels to the valence band ( $D^\circ, h$ ). Bound excitons are extrinsic transitions related to dopants or defects which create discrete electronic states in the band gap and therefore influence emission processes and optical transitions. In semiconductor material, in particular, the band structure strongly influences the electronic states of the bound excitons. Excitons could be, in theory bound to neutral or charged donors acceptors; however a basic assumption in the description of the bound exciton states for neutral acceptors and donors is a dominant coupling of the hydrogen-like particles in the bound- exciton (BE) states in the case of direct band gap materials.

### 2.1.2.3 Free-to-bound transitions (FB)

- A free conduction band electron can be bound to an acceptor as:  $e + A^0 \rightarrow (e, A^+) + h\nu$
- A free valence band hole can be bound to a donor as:  $h + D^0 \rightarrow (h, D^-) + h\nu$

The energy states of a bound exciton can be described as follows:

$$h\nu = E_g - E_{A/D} + \frac{k_B T}{2}$$

where  $h\nu$  is the photoluminescence peak energy of the  $(D^\circ, h)$  emissions,  $E_{A/D}$  is the ionization energy of the donor impurity. The shape of the luminescence spectrum of a free to bound (FB) transition can be determined by [42]

$$I(h\nu) \propto y^{1/2} \exp(-y) \text{ with } y = \frac{h\nu - E_g + E_{DA}}{k_B T}$$

where  $h\nu$  is the photoluminescence peak energy of the  $(e, A^\circ)$  emissions,  $E_A$  is the ionization of acceptor impurities,  $k$  is the Boltzmann's constant and  $T$  is the effective temperature of electrons in the conduction band which can be determined from the high-energy side of the experimental tail of the emission band. In general, with an increase in excitation power and temperature, the photoluminescence peak position of  $(e, A^\circ)$  emission shifts to higher energies. The shift in energy to increasing excitation power is due to band filling, while the shift in energy to increasing temperature can be offset by the band gap narrowing.

### 2.1.2.4 Donor- acceptor pair recombination (DAP)

A semiconductor is referred to as n- or p- type, when it may contain both donor and acceptor impurities according to the dominant impurity. These donors and acceptors can form pairs and act as stationary molecules imbedded in the host material.

The recombination energy of a donor- acceptor pair ( $D^0 + A^0 \rightarrow D^- + A^+ + h\nu$ ) is given by:

$$h\nu = E_g - (E_A + E_D) + \frac{e^2}{4\pi\epsilon_0\epsilon_r r} - E_{VdW}$$

where  $e$  is the electronic charge,  $\epsilon_r$  the static dielectric constant,  $r$  is the separation between donors and acceptors and  $E_{VdW}$  is a polarization interaction term dominated by the inter-center interaction in the initial state of the transition and the first order term,  $e^2/4\pi\epsilon_r$  is the Coulomb interaction between donor and acceptor impurities, and this term influences the binding energies of isolated impurities. Due to the Coulomb term the peak maximum energy of the donor acceptor emission shifts towards higher energies as the power excitation intensity,  $P_{exc}$ , increases, since with increasing power excitation the separation,  $r$ , between donors and acceptors is reduced 2.1.

$$h\nu_{DA}(P_{exc}) = h\nu_{DA}(P_0) + \beta \log_{10}(P_{exc}/P_0)$$

with the blue shift characterized by the factor  $\beta$  [ $meV/Dek$ ]. A blue shift is suggestive of donor- acceptor transitions (DAP)

### 2.1.3 Photon-related recombinations

The energy released from the recombination of an electron and hole can be transformed into photons and or optical phonons, the phonons being the collective vibrational modes of the atoms forming the crystal. The electron- phonon interaction can induce simultaneous emission of one or more phonons, leading to replicas or satellites of the main recombination peak in the photoluminescence spectrum displaced by the energies of the most important phonons, therefore strong phonon coupling can lead to the observation of multiple orders of phonon replicas.

- At the temperature  $T = 0K$  the shape of the emission band due to the phonon replicas is given by equation 2.1:

$$I_{em}(E) = I_0 \sum_n \frac{\exp(-S) S^n}{n!} \delta(E_0 - n\hbar\omega - E) \quad (2.1)$$

where  $S$  is the Huang- Rhys coupling factor representing the average number of phonons involved,  $E_0$  the energy of the zero-phonon transition, and  $I_0$  is the intensity in the zero-phonon line.

- At temperatures  $T > 0K$ , the term  $\exp(-S)$  tends to  $\exp(-S(1+2n))$  with  $n$  the mean thermal occupancy in the vibrational mode, given by the equation 2.2

$$n = \left[ \exp\left(\frac{\hbar\omega}{kT}\right) - 1 \right]^{-1} \quad (2.2)$$

and  $I_0$  becomes  $\exp(-S \coth(\frac{\hbar\omega}{2kT}))$  and decreases with increasing temperature. Additionally the zero-phonon line intensity tends to  $I_0 \exp(-S \coth(\frac{\hbar\omega}{2kT}))$ , when  $S$  is much less than unity, pointing out the fact that the sideband intensity increases with temperature as  $I_0 S \coth(\frac{\hbar\omega}{2kT})$ .

### 2.1.4 Experimental photoluminescence setup

Figure 2.1 illustrates the photoluminescence setup. The sample is excited with an argon ion ( $Ar^+$ ) laser (coherent Innova) with emission lines in the UV spectral range (330 to 360 nm), in the visible spectral range (450 to 514 nm), and with a semiconductor laser (668 nm). An helium cryostat (Oxford) was used to cool down the samples from room temperature 300 K to liquid helium temperature 4.2 K. A telescope system consisting of two lenses was used to collect photoluminescence signals into the scalable width (0.1 mm - 5 mm) entrance slit of a doubled grating monochromator with 0.22 m focal length. The resolution of the monochromator depends on its focal length, slit widths and the groove density of the grating. An OG 550 long pass orange filter placed between the telescope system and the entrance

slit of the monochromator was used to filter out the laser light which is much stronger than the fluorescence signal. The signal was detected with a Hamamatsu R 3236 nitrogen cooled photomultiplier tube placed at the exit slit of the monochromator. The detected signal is therefore filtered out and amplified by a lock-in-amplifier locked at the laser frequency of 170 Hz. Lock-in amplifiers are used to measure the amplitude and the phase of signals buried by noise. This is achieved by acting as a narrow bandpass filter, which removes much of the unwanted noise while allowing the signal which is to be measured to pass through. A reference must also be supplied to the lock-in. In this case chopper is used. Both the spectrometer and the photomultiplier tube voltage are controlled through a Labview program and the collected signal is recorded in a personal computer. In the measurements, the spectra obtained were corrected according to the spectral response of the double grating monochromator grating efficiency and to the photomultiplier tube quantum efficiency.

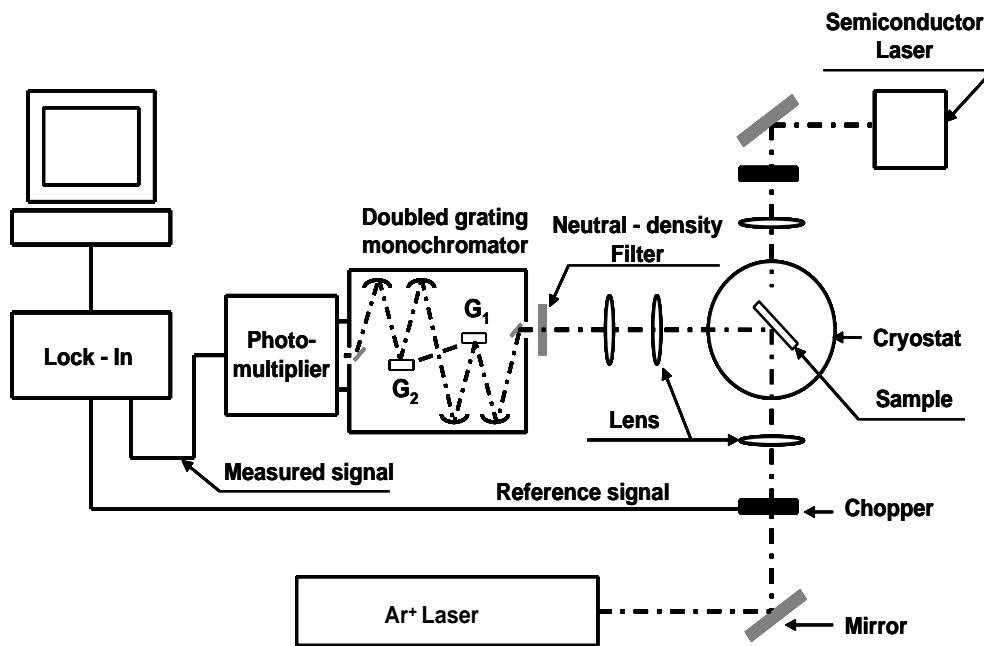


Figure 2.1: Layout of the photoluminescence spectroscopy setup

## 2.2 Electron Spin Resonance

### 2.2.1 Theory of paramagnetism

In an electron spin resonance (ESR) process, the degeneracy of the electron spin is lifted because of the interaction of the unpaired electron spin moment having an angular momentum  $\frac{1}{2}$  as measured in units of  $\hbar$ , with a magnetic field  $B_0$  (Zeeman effect). The energy level separation according to the elementary theory of the Zeeman effect is given by the equation 2.3:

$$\Delta E = g_e \mu_B B_0 \quad (2.3)$$

where for an electron spin the  $g_e$  factor or spectroscopic splitting factor is equal to 2.0023,  $\mu_B = e\hbar/2mc$  is the Bohr magneton, and  $B_0$  is the field strength of the external magnetic field. In ESR, the sample material immersed in a strong static magnetic field and exposed to an orthogonal microwave-frequency radiation (GHz) absorbs energy when the frequency of the radiation corresponds to the energy difference between two states of the electrons in the sample, and only when the transition satisfies the appropriate selection rules. The  $g$  value of the sample can be determined through the measurement of the absorption versus the magnetic field.

### 2.2.2 Experimental apparatus

Figure 2.2 displays a layout of an electron spin resonance apparatus. The E-580 ESR spectrometer (Bruker) consists of components that generate and detect microwave power, as well as an electromagnet with a current-regulated power supply to generate and modulate a uniform, static and homogeneous magnetic field of several thousand Gauss.

The microwave system consists of a microwave power supply (Gunn-Diode) operating at X-Band (9-10 GHz). The output of the microwave power supply, whose power level is adjusted with the attenuator, is routed via a rectangular waveguide towards a resonant cavity where the sample is mounted. The samples to be investigated are mounted in the middle of the cavity, where the magnetic component of the microwave power is oriented perpendicular to the static field and has a maximum. The detection of the microwaves is accomplished by a microwave diode situated inside the same box as the power supply. During the measurements, the higher the quality of the resonant cavity the greater the microwave field.

The detection of resonant ESR transitions carried out via a variety of schemes, the most popular being a detection of absorption of the microwave power. The solution to the signal-to-noise ratio problem is to introduce small-amplitude field modulation. An oscillating magnetic field is superimposed on the d.c. field by means of small coils, usually built into the cavity walls. When the field is close to a resonance line, it is swept forth and back through part of the line, leading to an a.c. component in the diode current. This a.c. component is amplified using a frequency selective amplifier, thus eliminating a great deal of noise. The modulation amplitude is normally less than the line width. Hence, the detected a.c. signal is proportional to the change in the sample absorption. In general the detected signal appears as a first derivative, since in order to minimize the noise from the microwave diode in the steady state measurements, a magnetic field modulation scheme with phase sensitive detection is generally used.

The range of the modulation frequency is 12 kHz to 100 kHz, and the amplitude of the field modulation can be varied up to 40 G in the Bruker spectrometer. The choice of the amplitude of field modulation should be appropriate, because if it is too large, the width of

the detected signal derivative would be wider than the real width of absorption, however the signal intensity would be less if the amplitude of field modulation is too small.

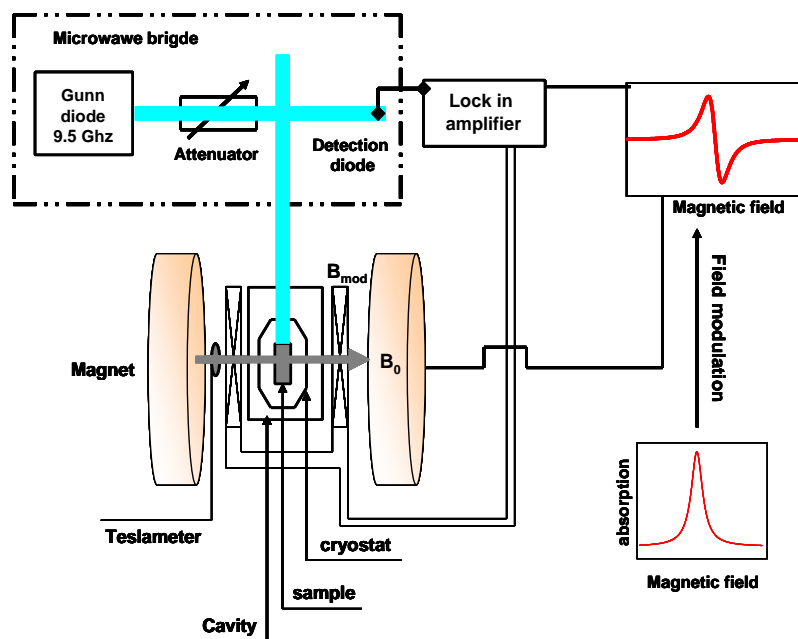


Figure 2.2: Layout of the Electron spin resonance setup

## 2.3 XRD

X-ray Diffraction (XRD) is a powerful technique used to identify the crystal phases present in material, to determine the thickness of thin films and multilayers and to measure the structural properties (phase composition, preferred orientation, defect structures) of these phases [43]. The crystalline structure of the  $\text{CuGaSe}_2$  films in this thesis was investigated using X-ray diffraction (XRD). In this technique, a monochromatic X-ray beam impinges on the surface of the sample and depending on the incidence angle, x-ray wavelength, and atomic spacing in the sample, constructive interference can occur in the diffracted beam. This phenomenon is explained by the Bragg relationship,

$$n\lambda = 2d \sin \theta$$

where  $n$  is an integer,  $\lambda$  is the wavelength,  $d$  is the crystal lattice spacing, and  $\theta$  is the angle of incidence. Patterns obtained from experiments were compared to Joint Committee on Powder Diffraction Spectra (JCPDS) data in order to identify crystalline phases and to determine whether the deposited films showed any degree of preferential orientation, based on the relative intensities of the diffraction peaks. For this study, the XRD system used was a Bruker D8 diffractometer with  $\text{Cu K}\alpha$  excitation ( $\lambda = 1.5418 \text{ \AA}$ ).

## 2.4 ERDA

Elastic recoil detection analysis (ERDA) technique using 230 MeV  $^{129}\text{Xe}$  ions as projectile was applied at the Ionenstrahllabor (ISL) of the Hahn-Meitner Institut Berlin to determine the absolute atomic concentration as a function of the film depth. The energy and time-of-flight of the scattered target atoms are measured simultaneously at a fixed path. The mass of elements are identified from the resulting scatter plot according to the relationship  $E = \frac{M}{2v^2}$  and the concentration of each element can be therefore determined from the measured number of the corresponding forward scattered specimen atoms.

## 2.5 SNMS

Focused  $\text{Ar}^+$  beam of  $E = 5$  keV and  $I \approx 1\mu\text{A}$  under an incident angle of  $60^\circ$  was used for sputtering. Two different sputter modes have been used:

- Stationary samples were cooled down to liquid nitrogen temperature
- Samples were rotated at room temperature.

The sputtered species were ionized by means of a cross- beam electron source of energy  $E = 50 - 80$  keV, whereby an electronic lens system assured that only atoms could reach the ionizer. Afterwards, the ionized atoms pass through a quadrupole mass spectrometer and are eventually detected by a Cu-Be-dynode. Secondary electrons emitted from the dynode were amplified by a photomultiplier and a preamplifier to a recordable signal. The concentration profiles are obtained by converting the raw data counts per seconds using experimentally determined sensitivity factors. These factors are based on system calibrations carried out on CIGS thin films and single crystals of well- known composition. A significant variation in total sputter rate as a function of sample composition was observed and a drop in sputter rate once the Mo back contact layer was reached. In order to eliminate the effect of film morphology and composition on the sputter rate, rotation of the samples during sputtering is required. All the SNMS spectra of this thesis were recorded at the ZSW (Zentrum für Solarenergie und Wasserstoff Forschung) Stuttgart Germany.